# Investigation of thermodynamic properties of $Cu(NH_3)_4SO_4 \cdot H_2O$, a Heisenberg spin chain compound

Tanmoy Chakraborty [a,b], Harkirat Singh [a,c], Dipanjan Chaudhuri [a,d], Hirale S. Jeevan [e], Philipp Gegenwart [e,f], Chiranjib Mitra [a,*]

[a] Indian Institute of Science Education and Research (IISER) Kolkata, Mohanpur Campus, PO: BCKV Campus Main Office, Mohanpur – 741252, Nadia, West Bengal, India
[b] Fakultät Physik, Technische Universität Dortmund, D-44221 Dortmund, Germany
[c] Tata Institute of Fundamental Research, Homi Bhabha Road, Colaba, Mumbai 400 005, India
[d] The Institute for Quantum Matter, Department of Physics and Astronomy, The Johns Hopkins University, Baltimore, MD 21218, USA
[e] I. Physikalisches Institut, Georg-August-Universitat, D-37073 Göttingen, Germany
[f] Experimental Physics VI, Center for Electronic Correlations and Magnetism, University of Augsburg, 86159 Augsburg, Germany

## 1. Introduction

In recent times, numerous successful efforts have been devoted to explore spin systems with low dimensional magnetic interactions. Many low dimensional spin systems could be suitably described by physical models there by enabling us to capture essential experimental manifestations [1–6]. For instance, dimerized and uniform spin ½ chain, spin ladder, frustrated spin systems etc. are some of the well-studied models where the theoretical predictions have been verified experimentally [2,4,5]. Insights into the physics of low dimensional spin systems have been gained using powerful numerical techniques like Quantum Monte Carlo (QMC) simulations [7,8], Exact Diagonalization (ED) [9] and Transfer Matrix Renormalization Group (TMRG) [10] technique on one hand, whereas on the other hand, analytical methods like field-theoretical approaches [11] and Bethe ansatz [12] have been employed. Successful preparation of the materials which are representative of different spin models, allows researchers to verify different thermodynamic properties predicted using the above theoretical tools. Thus a fruitful connection has been established between theory and experiment [1–6,13]. Low dimensional spin systems have attracted attention of an immense number of researchers, mainly due to the fact that the ground states of these systems show a number of unique features. For instance, a Heisenberg spin chain, exhibiting an entangled ground state, contributes to non-zero entanglement even at finite temperatures being in a weighted thermal mixture of ground and excited states [14]. Other novel characteristics include spin-gap excitation using far-infrared spectroscopy [15], exotic thermal and spin transport properties at finite temperature [16], magnetic singlet bound states using light scattering experiments [17] etc. Thus, magnetic materials, whose behaviors resemble the proposed theoretical models, have provided a platform for investigating these exotic features extensively.

Low dimensional quantum spin ½ systems exhibit interesting magnetic and thermal properties. A well-known Spin-Peierls compound $CuGeO_3$, which possesses a dimerized spin state below a critical temperature $T_c = 14$ K, has shown a direct evidence for singlet-triplet transition through inelastic neutron scattering

* Corresponding author.
*E-mail addresses:* tanmoy.chakraborty@tu-dortmund.de (T. Chakraborty), chiranjib@iiserkol.ac.in (C. Mitra).

experiment [18,19]. Another well studied spin ½ compound τ-$(BEDT\text{-}TTF)_2Cu_2(CN)_3$, which exemplifies an organic Mott insulator with frustrated quantum spins, have been modeled by a triangular-lattice Heisenberg system with exchange coupling constant $J \sim 250$ K as corroborated by $^1H$ NMR and static susceptibility measurements [20]. $TlCuCl_3$, $BaCuSi_2O_6$ and $Cu(NO_3)_2\text{-}2.5D_2O$ are three extensively studied dimerized quantum antiferromagnets where quantum phase transition and Bose-Einstein condensation of magnons have been experimentally observed ([21] and references therein). $SrCu_2(BO_3)_2$ is another widely investigated compound showing evidence for localized singlet-triplet excitation and it also represents the Shastry-Sutherland model of a 2D spin-gap system with the ground state of a dimer [22]. The class of spin ½ Heisenberg chain materials belonging to the family of low dimensional systems, has fascinated many researchers in last few decades. For example, $CuSe_2O_5$ [23] and $KCuGaF_6$ [24] have demonstrated promising experimental results and a striking match with theoretical calculations. $Sr_2CuO_3$, another 1D isotropic antiferromagnetic spin chain with extremely large exchange coupling constant (~1300 K), shows spin-orbital separation as it has been reported recently [25]. Furthermore, a thorough investigation of thermodynamic properties for $Cu(C_4H_4N_2)(NO_3)_2$ and $[Cu(\mu\text{-}C_2O_4)(4\text{-}aminopyridine)_2(H_2O)]_n$ have established them as good realization of spin ½ Heisenberg chain [26,27].

In the present work, we have experimentally studied detailed magnetic and thermal properties of such an antiferromagnetic uniform spin ½ chain with isotropic Heisenberg interaction. The Hamiltonian for the system in presence of applied external magnetic field can be written as,

$$H = \frac{J}{4}\sum_i [\alpha\sigma_i^z\sigma_{i+1}^z + \beta(\sigma_i^x\sigma_{i+1}^x + \sigma_i^y\sigma_{i+1}^y)] + g\mu_B B\sum_i \sigma_i^z \qquad (1)$$

where $0 \le \alpha \le 1$, $0 \le \beta \le 1$, $B$ is the external magnetic field, $\sigma^x, \sigma^y, \sigma^z$ are the three Pauli spin matrices, $g$ is the Landé g factor, $\mu_B$ is the Bohr Magneton and $J$ is the exchange coupling constant. The summation is taken over nearest neighboring spins. The compound we have studied in the present work, is $Cu(NH_3)_4SO_4{\cdot}H_2O$ which could be described by isotropic Heisenberg model with $\alpha = \beta = 1$ in Eq. (1) [28,29]. Jong et al. reported the experimental results for the present compound and described it as an exchange coupled Heisenberg spin chain [4]. Zero field magnetic susceptibility data as a function of temperature has shown the existence of a broad maximum around 3.5 K whereas the temperature dependent specific heat curve has shown a peak around 3 K [4,28,29]. These thermal and magnetic measurements have ascertained the existence of magnetic interaction along a particular direction in $Cu(NH_3)_4SO_4{\cdot}H_2O$ [4,28,29]. The crystallographic structure analysis reported by F. Mazzi has revealed the spin chain behavior in $Cu(NH_3)_4SO_4{\cdot}H_2O$ [30]. In a linear chain, $Cu^{++}$ ions are connected along the c axis as – $Cu^{++}$–$H_2O$– $Cu^{++}$– $H_2O$– while the $Cu^{++}$ ions of neighboring chains are connected as – $Cu^{++}$–$NH_3$–$SO_4$–$NH_3$– $Cu^{++}$–, which results in larger intrachain coupling strength in comparison to that between the chains. Interaction with next nearest neighboring spins along the chain is also negligible here.

A detailed estimation of various thermodynamic quantities using the experimental data has been presented in the paper with the following order. Temperature dependence of magnetic susceptibility and field dependence of isothermal magnetization are measured and compared with the solution for isotropic Heisenberg spin ½ chain. Heat capacity data are collected both at zero magnetic field and externally applied field, and compared with the Bethe ansatz solution for spin ½ chain. Finally, zero field and field dependent specific heat data were used to estimate internal energy and entropy.

## 2. Experimental details

We have measured single crystalline $Cu(NH_3)_4SO_4{\cdot}H_2O$ of purest grade (99.999%), supplied by Sigma Aldrich. Magnetic susceptibility and magnetization measurements are performed in a Magnetic Property Measurement System (MPMS) from Quantum Design and Vibrating Sample Magnetometer (VSM) from Oxford. Temperature dependence of static magnetic susceptibility is measured in a temperature range of 1.9–30 K. Subsequently, isothermal magnetization measurements are carried out as a function of magnetic field at various temperatures. The field is varied from 0T to 14T and the temperature is varied from 1.9 K to 10 K.

The specific heat measurements are performed by standard relaxation method in a Physical Property Measurement System (PPMS) from Quantum Design. Zero field specific heat data are collected in a temperature range of 2–10 K. Furthermore, field dependent specific heat is measured in the same temperature range. The magnetic field is varied from 0T to 7T. Careful subtraction of background is performed by carrying out addenda measurement before starting the experiments.

## 3. Results and discussions

Fig. 1 displays experimental magnetic susceptibility as a function of temperature. The plot shows that the susceptibility curve has a rounded maximum at $T_{max} = 3.7$ K which is quite close to the earlier reported value [28]. When the temperature is increased beyond 3.7 K, the susceptibility gradually decreases. This is an indicative of antiferromagnetic linear chain behavior [6]. Previously reported results have satisfactorily established an evidence of isotropic Heisenberg interaction in $Cu(NH_3)_4SO_4{\cdot}H_2O$ between the neighboring spins along the chains of $Cu^{++}$ ions [31,32]. Bonner and Fisher employed the exact diagonalization technique to calculate the magnetic susceptibility for antiferromagnetic spin chain where they varied the number of spins up to 11. However, due to the finite size effect, their result cannot satisfactorily explain the experimental data for an infinite chain. Subsequently, by following the analytical approach by Bethe ansatz [12], it was possible to solve the one dimensional Heisenberg spin ½ model exactly [33,34] down to sufficiently low temperature. The solution has been efficiently applied to analyze the thermodynamic behavior of certain spin chain materials [26,27]. Since the present system is a representative of uniform isotropic chain model where the

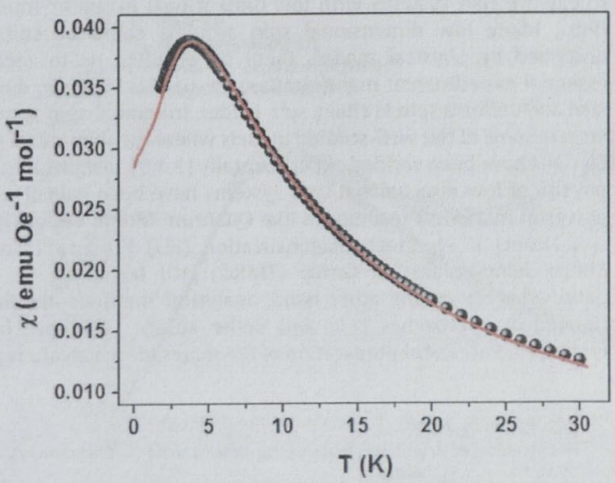


**Fig. 1.** Magnetic susceptibility versus temperature for $Cu(NH_3)_4SO_4{\cdot}H_2O$ (circles represent the experimental data while the exact solution of the S = 1/2 Heisenberg model using J = 6 and g = 2.056 is shown by the solid red curve).

neighboring spins of the constituent $Cu^{++}$ ions being arranged in a periodic fashion along one particular direction, we compare the exact result for susceptibility derived by Bethe ansatz technique for infinite spin ½ chain with the experimental data. We have analyzed the data in the temperature range of 1.9–30 K as shown in Fig. 1. The best match was found for exchange coupling constant J = 6 K and Landé g factor g = 2.056. The theoretical curve (solid red line) appears to be consistent with the experimental data (open circles).

Isothermal magnetization data are recorded at low temperature regime where the antiferromagnetic correlations survive persistently. The magnetization curves taken at 1.9 K, 2.5 K and 3.4 K (which are above the antiferromagnetic ordering temperature 0.37 K [32]) are plotted in Fig. 2 with magnetic field varying from 0T to 14T along the horizontal axis. It can be seen that the magnetization curve at lowest temperature (1.9 K) almost reaches its saturation value at 14T. ALPS (Algorithms and Libraries for Physics Simulations) provide simulation codes for various strongly correlated quantum mechanical models [35]. Based on the "stochastic series expansion in the directed loop representation" method [36], QMC technique is employed (using code from ALPS) to simulate isothermal magnetization curves for N = 100 spin ½ sites. This analysis is performed for all the three above mentioned experimental isotherms. The simulated curves are plotted in the same graph with the experimental ones. It is evident from the graph that the experimental curves are in well agreement with the corresponding simulated ones (assuming J = 6.8 K). A small mismatch can be observed between the simulation and experiment both at low and high magnetic field values. This discrepancy can happen due to the fact that the spin chain compound may contain paramagnetic spins due the boundary effect of the spin chains and other magnetic impurities which also contribute to the magnetization curve, whereas the simulation represents an exact solution for a spin ½ chain with 100 sites. Subsequently, all the experimental magnetization isotherms (from 1.9 K to 10 K) are used to generate a 3D plot with magnetization, magnetic field and temperature along the three axes. The plot is shown in Fig. 3. This plot more explicitly depicts the variation of magnetization with field and temperature.

Experimental specific heat data for $Cu(NH_3)_4SO_4{\cdot}H_2O$ single crystals measured in absence of external magnetic field in a temperature range of 2–10 K is shown in Fig. 4 (open circles). The most prominent feature in the data that can be observed is the appearance of a broad maximum at $T_{max}$ = 3 K which matches well with previous results [28,29]. Upon enhancement of temperature, the specific heat decreases. However, when the temperature is increased further, an upturn in the specific heat curve is observed which happens solely due to the lattice contribution which will be clear from the ensuing analysis. The temperature dependence of specific heat can be represented by the following relation,

$$C(T) = C_m(T) + \beta T^3 \tag{2}$$

Here $C_m$ is the magnetic specific heat and the lattice contribution is determined by the coefficient $\beta$. We have used the Bethe ansatz result for specific heat [33] for the case of isotropic Heisenberg chain model to analyze the magnetic part of the experimental specific heat data. Experimental values of $C_m(T)$ have been extracted by subtracting the lattice part from $C(T)$ and plotted with temperature in Fig. 4 (open squares). Subsequently, the numerical data calculated by Bethe ansatz technique was compared with the

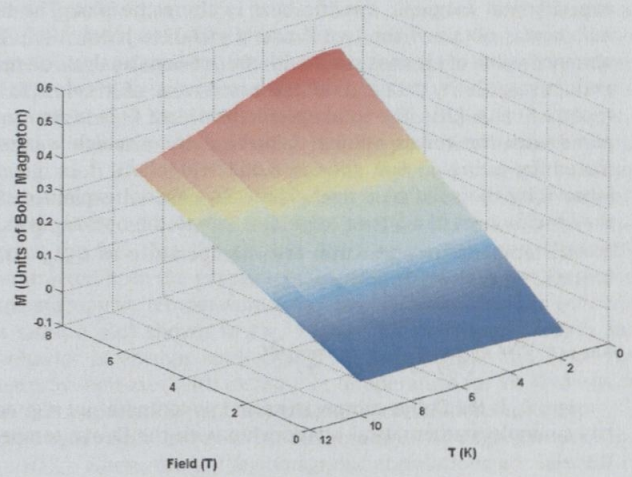


**Fig. 3.** Surface plot with magnetization, magnetic field and temperature along the three axes.

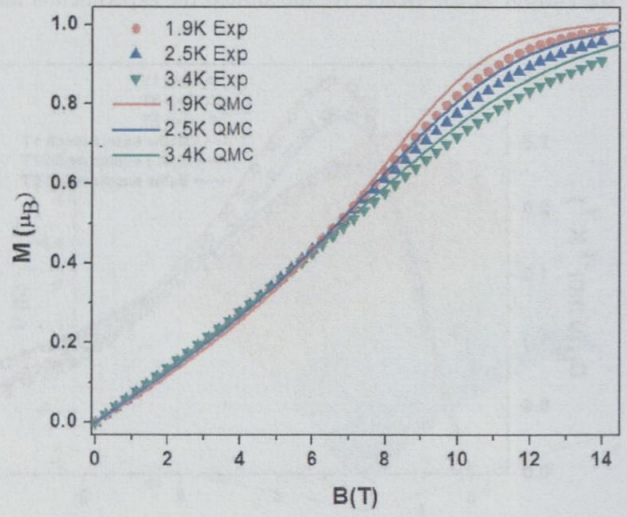


**Fig. 2.** Experimental magnetization vs. magnetic field data at different temperature values (symbols represent data taken at temperatures shown in the legend) along with the corresponding QMC (Quantum Monte Carlo) results derived using the Hamiltonian for a chain consisting of 100 spins.

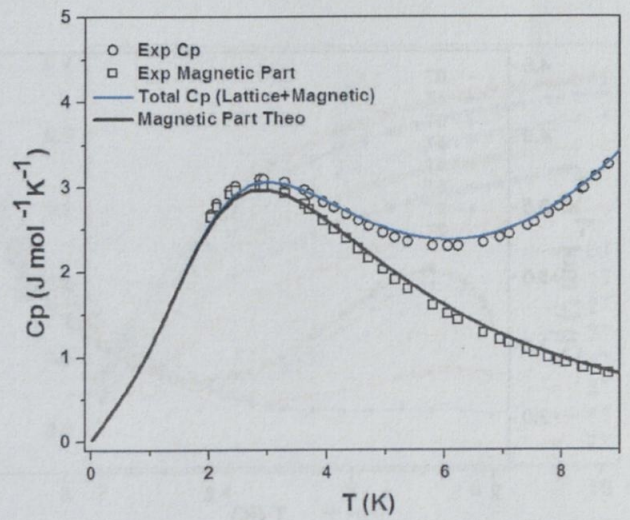


**Fig. 4.** Total (magnetic and lattice component) and magnetic (see legend) specific heat data for $Cu(NH_3)_4SO_4{\cdot}H_2O$. Solid curves are the respective calculated curves as shown in the legend and explained in the main text.

experimental magnetic specific heat in the same plot. The best match was obtained for J = 6 K and $\beta = 0.00218\ \mathrm{J\,Mol^{-1}\,K^{-4}}$. The obtained value of J is consistent with the previous analysis on magnetic susceptibility data and the estimated value of $\beta$ is close to the reported value [28]. The total specific heat data $C(T)$ is also compared with the corresponding theoretical curve which was estimated by using $J = 6$ K and $\beta = 0.00218\ \mathrm{J\,Mol^{-1}\,K^{-4}}$ in Eq. (2) (shown by the solid blue line). The Debye model explained that the specific heat of a lattice originates due to the optical phonons at low temperature and varies with temperature as $C_{Debye} = \beta T^3$. This can be derived from the equation [37]

$$C_{Debye} = 9NK_B\left(\frac{T}{\theta_D}\right)\int_0^{T/\theta_D}\frac{x^4e^x}{(e^x-1)^2}dx. \tag{3}$$

Here $\theta_D$ is the Debye temperature. In low temperature regime, $\beta$ has a simple mathematical relationship with the Debye temperature $\theta_D$.

$$\beta = 12\pi^4NK_B/5\theta_D^3. \tag{4}$$

Estimation of Debye temperature was performed by substituting $\beta = 0.00218$ in the above equation. We obtained $\theta_D = 96.27$ K for the present compound. The notable characteristic of the specific heat curve is the broad peak around 3 K which arises due to the intrinsic contribution from the many-level energy spectrum of the Heisenberg spin chain [37]. At very low temperature, the thermal energy is not sufficient to excite the system to the higher energy states, yielding a very low value of specific heat. However, with increase in temperature, the probability of excitation to the higher energy states increases and the specific heat starts rising. When the rate of absorption of thermal energy reaches its peak value, specific heat curve shows a maximum which happens around 3 K. Upon further increasing the temperature, the specific heat drops down to lower value as the energy levels become populated equally and no differential change in the internal energy occurs.

Fig. 5 displays experimental specific heat $C(T)$ data from 2 K to 10 K in presence of magnetic field up to 7T. Upon increasing the field, the broad maximum at 3 K is suppressed towards lower temperature and completely disappears around 5T. This behavior is quite similar to the experimental results obtained in the case of other uniform spin chain materials [26,27]. Bonner and Fisher numerically estimated specific heat for isotropic Heisenberg case where the number of the spins was varied from 2 to 11 [38]. Later, A. Klümper investigated the thermodynamics of infinite spin ½ Heisenberg chain and calculated specific heat as a function of temperature at different applied magnetic field values [39]. They observed that with increasing field the maxima in the $C(T)$ vs. $T$ curves shifts towards lower temperature regime accompanied by a reduction in height which supports our experimental data. In order to analyze the field dependent specific heat data, we have employed the numerical $C(T)$ vs. $T$ datasets (at different applied fields) derived by A Klümper using the Bethe ansatz [39]. The experimental data and the exact solution (the theoretically generated curves have been scaled by assuming J = 6 K) for 1T, 3T and 5T are plotted in the same graph. One can conclude that the experiment and theory are quite consistent with one another (Fig. 6). Measured specific heat vs. temperature datasets at constant fields were used to create the 3D plot shown in Fig. 7.

Next, fundamental thermodynamic quantities, namely, internal energy and entropy are quantified for $Cu(NH_3)_4SO_4{\cdot}H_2O$ from the experimental specific heat data. In general, the internal energy at some particular temperature $T$ is related to the specific heat by the following equation

$$U(T) = U_{2K} + \int_{2K}^{T} C(T')dT' \tag{5}$$

with $U_{2K}$ being the internal energy at 2 K. Numerical integration is carried out on the specific heat data in the temperature range of 2–10 K and the above mentioned integral equation is used to quantify experimental internal energy for the present compound. The analysis is performed for each field dependent magnetic specific heat datasets. In order to determine $U_{2K}$, the theoretical treatment of A. Klümper is followed [39,40]. We have used J = 6 K obtained from earlier analyses. Thus, the theoretical values of internal energy $U_{2K}$ at the particular fields corresponding to the experimental $C_m(T)$ vs. $T$ datasets are substituted in the integral equations (5) to evaluate temperature dependent internal energy datasets [$U(T)$ vs. $T$ ] at different fixed fields. Both the theoretical and the experimental energies are scaled in the unit of Kelvin. Evaluated $U(T)$ vs. $T$ datasets are plotted in Fig. 8. A surface plot has been created using the $U(T)$ vs. $T$ datasets for different fields (Fig. 9).

Fundamental thermodynamic relations imply that the entropy increment of a system could be simply calculated from specific heat using the relation $\Delta S(T) = S_{2K} + \int_{2K}^{T}[C(T')/T']dT'$. Here $S_{2K}$ is the entropy at 2 K. Hence, we substituted the experimental mag-

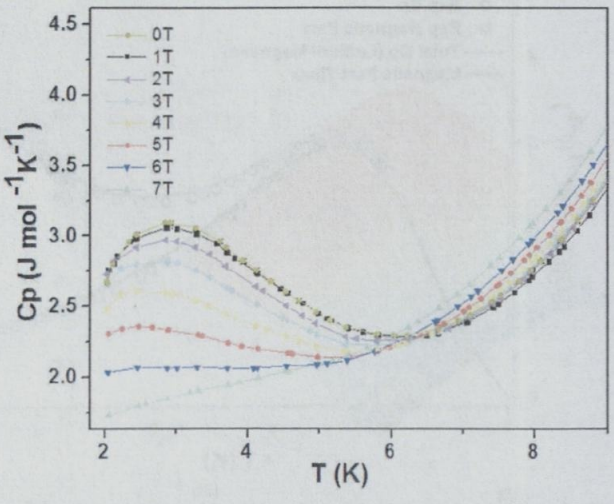


**Fig. 5.** Experimental specific heat data for $Cu(NH_3)_4SO_4{\cdot}H_2O$ as a function of temperature at different fields.

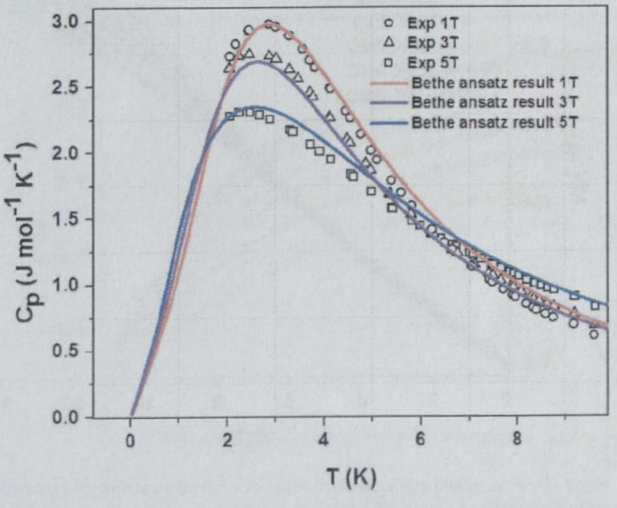


**Fig. 6.** Comparison of experimental specific heat data with corresponding Bethe ansatz results for magnetic fields of 1T, 3T and 5T.

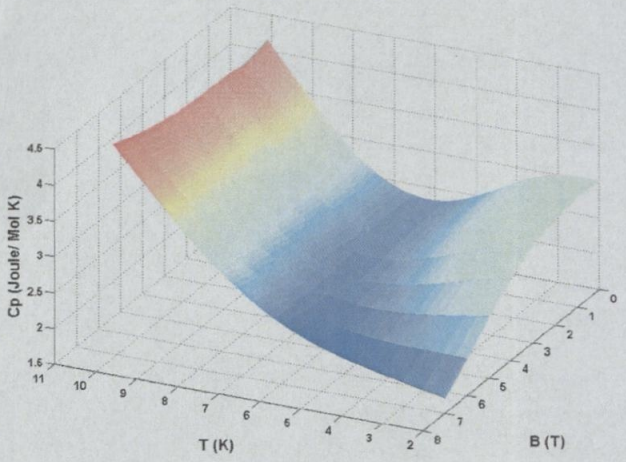


**Fig. 7.** Three dimensional plot depicting the variation of experimental specific heat with magnetic field and temperature.

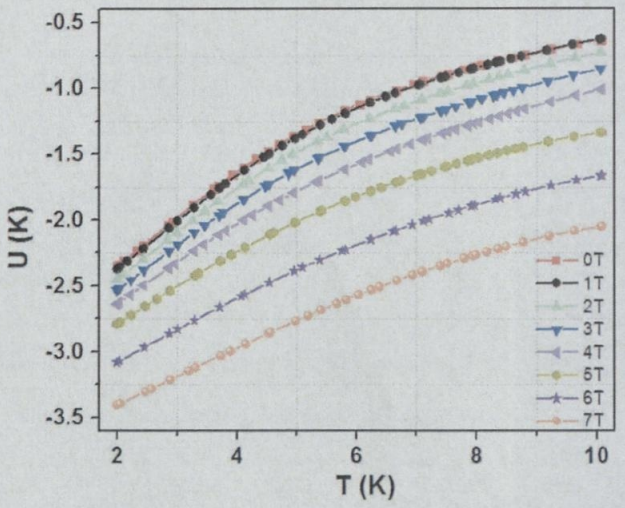


**Fig. 8.** Variation of experimental internal energy with temperature for different applied magnetic fields (as shown in the legend).

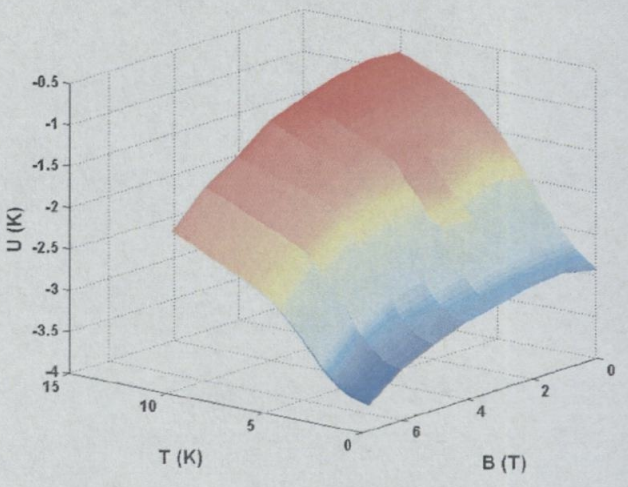


**Fig. 9.** Three dimensional variation of internal energy with magnetic field and temperature along the other two axes.

netic specific heat data in the above equation and integrated numerically to estimate the entropy increment. The above treatment was performed for all $C_m(T)$ vs. $T$ datasets obtained at fixed fields and these results are shown in Fig. 10. The integration constant (entropy for S = 1/2 Heisenberg spin chain at T = 2 K) has been determined theoretically [39,40] and incorporated in the integration. The figure shows that the zero field magnetic entropy saturates at the value of 0.688 which is quite close to the theoretically predicted value of ln(2) = 0.693. This observation also supports the fact that the phonon contribution has been efficiently subtracted from the experimental specific heat data. We then used the entropy vs. temperature datasets at different fields to generate a surface plot shown in Fig. 11. The plot explicitly depicts the behavior of entropy with change in temperature and field. The entropy increases with increase in temperature for all field values as it is expected for antiferromagnetic correlations or ordering is destroyed with increase in temperature. At high temperature (~10 K), where the antiferromagnetic correlations are minimum, the entropy decreases upon increasing the field because of field dependent alignment of the paramagnetic spins.

## 4. Conclusion

The present work exemplifies an investigation of thermodynamics of a Heisenberg spin ½ chain material where an intimate detail about the system has been captured. In summary, we have performed a study of thermal and magnetic properties of Cu $(NH_3)_4SO_4{\cdot}H_2O$ which can be described by an ideal spin ½ chain with isotropic Heisenberg interaction. Temperature dependent susceptibility and specific heat data have been compared with the results calculated using the Bethe ansatz technique. The experimental data are in excellent agreement with the calculation using an exchange coupling constant J = 6 K. This consistency indicates that the material displays spin chain behavior in the temperature regime down to 2 K. Field dependent magnetization curves are generated numerically using QMC technique at the Heisenberg extreme. Numerically simulated curves are in agreement with the experimental ones. Temperature dependent specific heat data at various applied fields are also compatible with the exact results for infinite Heisenberg spin chain. Furthermore, numerical integration is performed on the experimental specific heat data to obtain the variation of internal energy and entropy with temperature at different fields.

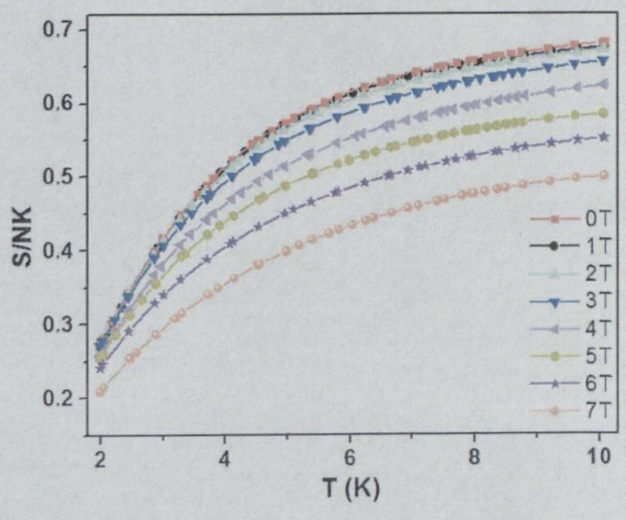


**Fig. 10.** Temperature dependence of entropy obtained from the experimental specific heat data taken at different fields (as shown in the legend).

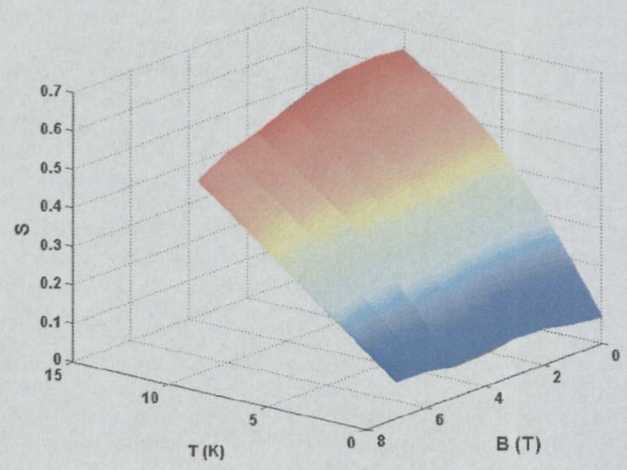


**Fig. 11.** Three dimensional plot of entropy with magnetic field and temperature.

These spin chain systems can have fruitful applications in quantum communications. Bose has described that an entangled spin chain can be used as an appropriate channel for transmitting a quantum state over a short distance [41]. It has been suggested that the above scheme can be efficiently implemented for one-dimensional Heisenberg chain compounds with nearest neighboring interaction where a quantum state can be transferred with an improved fidelity compared to the classical one [41]. Successful implementation of the above protocol can play a significant role in designing a feasible quantum computer. Moreover, the possibility of having entangled spins in solid state crystals has an advantage over the optical systems as the crystals can be efficiently integrated with existing Si-based technology or other quantum devices [42].

## Acknowledgments

The authors would like to thank the Ministry of Human Resource and Development, Government of India and Göttingen Kolkata Open Shell Systems (G-KOSS) for funding. We sincerely acknowledge A. Honecker for useful discussions. The authors are grateful to S. K. Dhar for allowing us to carry out the isothemal magnetic measurements in his lab in TIFR, Mumbai. We also acknowledge K. R. Kumar and A. Maurya for their assistance with the magnetic measurements.

## References

[1] T.M. Rice, Z. Phys. B 103 (1997) 165.
[2] E. Dagotto, Rep. Prog. Phys. 62 (1999) 1525.
[3] E. Dagotto, T.M. Rice, Science 271 (1996) 618.
[4] L.J.D. Jongh, A.R. Miedema, Adv. Phys. 23 (1974) 1.
[5] M. Hase, I. Terasaki, K. Uchinokura, Phys. Rev. Lett. 70 (1993) 3651.
[6] D.C. Johnston, R.K. Kremer, M. Troyer, X. Wang, A. Klümper, S.L. Budko, A.F. Panchula, P.C. Canfield, Phys. Rev. B 61 (2000) 9558.
[7] M. Troyer, F. Alet, S. Trebst, S. Wessel, AIP Conf. Proc. 690 (2003) 156.
[8] H.G. Evertz, Adv. Phys. 52 (2003) 1.
[9] N. Laflorencie, D. Poilblanc, Lect. Notes Phys. 645 (2004) 227.
[10] U. Schollwöck, Rev. Mod. Phys. 77 (2005) 259.
[11] D.C. Cabra, P. Pujol, Lect. Notes Phys. 645 (2004) 253.
[12] H. Bethe, Z. Phys. 71 (1931) 205.
[13] D.C. Johnston, M. Troyer, S. Miyahara, D. Lidsky, K. Ueda, M. Azuma, Z. Hiroi, M. Takano, M. Isobe, Y. Ueda, M.A. Korotin, V.I. Anisimov, A.V. Mahajan, L.L. Miller, Magnetic Susceptibilities of Spin-1/2 Antiferromagnetic Heisenberg Ladders and Applications to Ladder Oxide Compounds Preprint cond-mat/0001147, 2000.
[14] L. Amico, R. Fazio, A. Osterloh, V. Vedral, Rev. Mod. Phys. 80 (2008) 517;
M. Wiesniak, V. Vedral, C. Brukner, Phys. Rev. B 78 (2008) 064108.
[15] T. Rööm, D. Hüvonen, U. Nagel, Phys. Rev. B 69 (2004) 144410.
[16] F. Heidrich-Meisner, A. Honecker, D.C. Cabra, W. Brenig, Phys. Rev. B 66 (2002) 140406(R).
[17] P. Lemmens, G. Güntherodt, C. Gros, Phys. Rep. 375 (2003) 1.
[18] K. Hirota, D.E. Cox, J.E. Lorenzo, G. Shirane, J.M. Tranquada, M. Hase, K. Uchinokura, H. Kojima, Y. Shibuya, I. Tanaka, Phys. Rev. Lett. 73 (1994) 736.
[19] O. Fujita, J. Akimitsu, M. Nishi, K. Kakurai, Phys. Rev. Lett. 74 (1995) 1677.
[20] Y. Shimizu, K. Miyagawa, K. Kanoda, M. Maesato, G. Saito, Phys. Rev. Lett. 91 (2003) 107001.
[21] T. Giamarchi, C. Rüegg, O. Tchernyshyov, Nature 4 (2008) 198.
[22] H. Kageyama, K. Yoshimura, R. Sten, N.V. Mushnikov, K. Onizuka, M. Kato, K. Kosuge, C.P. Slichter, T. Goto, Y. Ueda, Phys. Rev. Lett. 82 (1999) 3168;
H. Kageyama, M. Nishi, N. Aso, K. Onizuka, T. Yosihama, K. Nukui, K. Kodama, K. Kakurai, Y. Ueda, Phys. Rev. Lett. 84 (2000) 5876.
[23] O. Janson, W. Schnelle, M. Schmidt, Y. Prots, S. Drechsler, S.K. Filatov, H. Rosner, New J. Phys. 11 (2009) 113034.
[24] I. Umegaki, H. Tanaka, T. Ono, H. Uekusa, H. Nojiri, Phys. Rev. B 79 (2009) 814401.
[25] T. Ami, M.K. Crawford, R.L. Harlow, Z.R. Wang, D.C. Johnston, Q. Huang, R.W. Erwin, Phys. Rev. B 51 (1995) 5994;
J. Schlappa, K. Wohlfeld, K.J. Zhou, M. Mourigal, M.W. Haverkort, V.N. Strocov, L. Hozoi, C. Monney, S. Nishimoto, S. Singh, A. Revcolevschi, J.-S. Caux, L. Patthey, H.M. Rønnow, J. van den Brink, T. Schmitt, Nature 485 (2012) 82.
[26] B. Wolf, Y. Tsui, D. Jaiswal-Nagar, D. Tutsch, A. Honecker, K. Remović-Langer, G. Hofmann, A. Prokofiev, W. Assmus, G. Donath, M. Lang, Proc. Natl. Acad. Sci. 108 (2011) 6862.
[27] P.R. Hammar, M.B. Stone, D.H. Reich, C. Broholm, P.J. Gibson, M.M. Turnbull, C. P. Landee, M. Oshikawa, Phys. Rev. B 59 (1999) 1008.
[28] R.B. Griffiths, Phys. Rev. 135 (3A) (1964) A659.
[29] T. Haseda, A.R. Miedema, Physica 27 (1961) 1102.
[30] F. Mazzi, Acta. Cryst. 8 (1955) 137.
[31] J.J. Fritz, H.L. Pinch, J. Am. Chem. Soc. 79 (1957) 3644.
[32] T. Oguchi, Phys. Rev. 133 (4A) (1964) A1098.
[33] A. Klümper, D. Johnston, Phys. Rev. Lett. 84 (2000) 4701.
[34] S. Eggert, I. Affleck, M. Takahashi, Phys. Rev. Lett. 73 (1994) 332.
[35] A.F. Albuquerque et al., J. Magn. Magn. Mater. 310 (2007) 1187;
B. Bauer et al., J. Stat. Mech. 2011 (2011) P05001.
[36] A.W. Sandvik, Phys. Rev. B 59 (1999) 14157;
F. Alet, S. Wessel, M. Troyer, Phys. Rev. E 71 (2005) 036706;
L. Pollet, S.M.A. Rombouts, K. Van Houcke, K. Heyde, Phys. Rev. E 70 (2004) 056705.
[37] E.S.R. Gopal, Specific Heats at Low Temperatures, Plenum Press, New York, 1966.
[38] J.C. Bonner, M.E. Fisher, Phys. Rev. 135 (3A) (1964) A640.
[39] A. Klümper, Eur. Phys. J. B 5 (1998) 677.
[40] C. Trippe, A. Honecker, A. Klümper, V. Ohanyan, Phys. Rev. B 81 (2010) 054402.
[41] S. Bose, Phys. Rev. Lett. 91 (2003) 207901.
[42] L.G. Herrmann, F. Portier, P. Roche, A.L. Yeyati, T. Kontos, C. Strunk, Phys. Rev. Lett. 104 (2010) 026801.